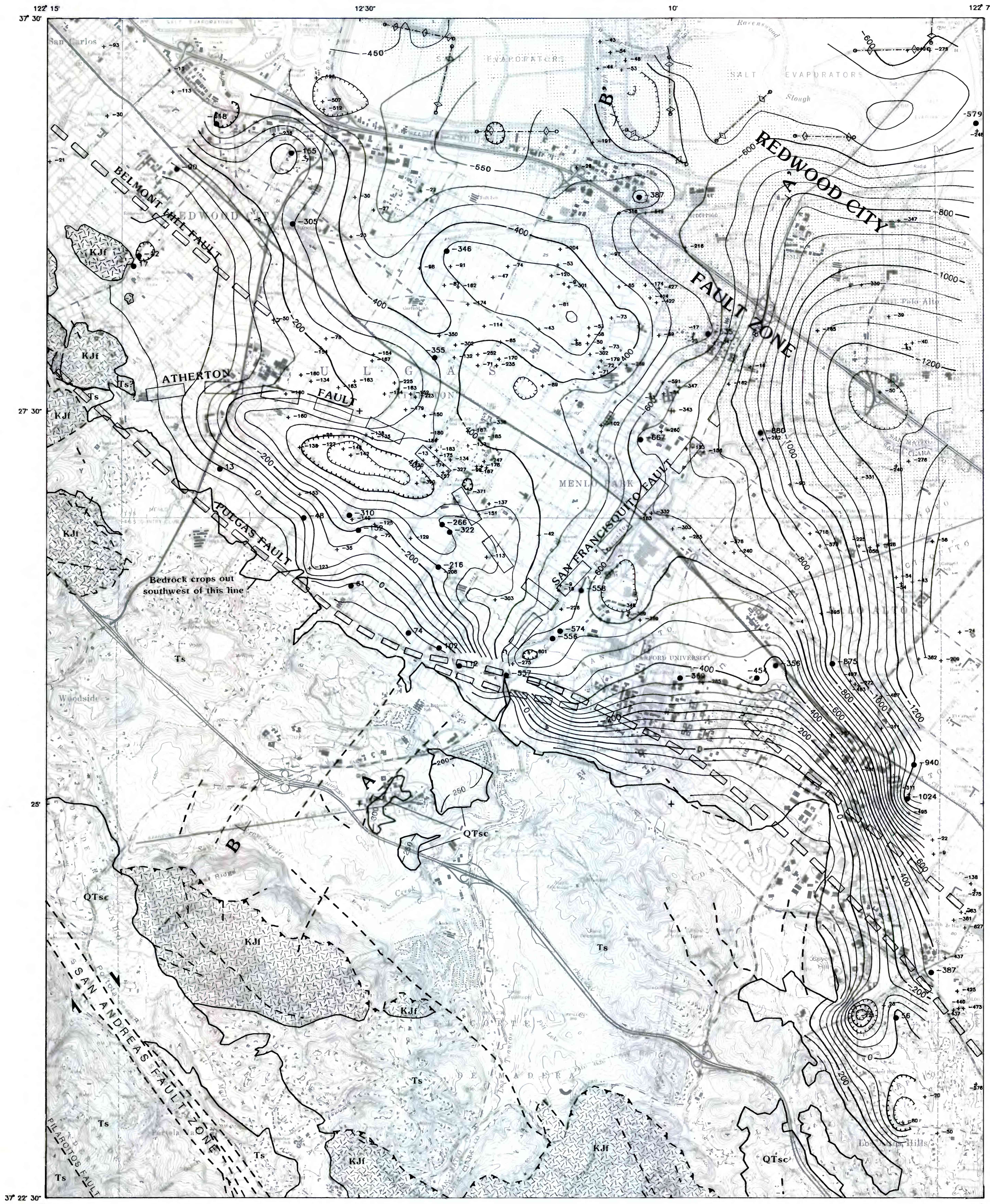

Base from U.S. Geological Survey Palo Alto 7.5' quadrangle 1:24,000 1961 (revised 1968, 1973)
1000-meter Universal Transverse Mercator grid ticks, zone 10

SCALE 1:24000

Geologic base from Pampeyan (1970)

AREA OF MAP

SHEET 3. GEOPHYSICAL INTERPRETATIVE MAP OF BEDROCK SURFACE BENEATH THE FLATLAND AREAS OF MENLO PARK, ATHERTON AND ADJOINING AREAS, CALIFORNIA

By
Steven F. Carle, V. E. Langenheim, Earl E. Brabb and Earl H. Pampeyan

PRELIMINARY GROUND WATER QUALITY DATA AND THE EXTENT OF THE GROUND WATER BASIN FROM DRILL HOLE, SEISMIC, AND GRAVITY DATA IN THE PALO ALTO 7.5' QUADRANGLE, CALIFORNIA

Howard W. Oliver
Editor

1990

EXPLANATION

Contours on bedrock beneath and older than Santa Clara Formation (upper Pliocene and lower Pleistocene), showing elevation in feet above or below mean sea level. Contour interval 50 feet. Barbed lines enclose low areas.

● −387 Elevation of bedrock surface and location of well that penetrates bedrock.

+ −425 Elevation of bottom of well that did not penetrate bedrock.

Seismic refraction profiles reported by Hazlewood (1976). " " indicates end points of lines; locality where elevation of bedrock used to plot contours on this map.

Geologically inferred fault.

Geophysically inferred fault.

Fault--dashed where approximately located.

Geophysically inferred fault zone.

QTsc — Santa Clara Formation (upper Pliocene and lower Pleistocene) and undivided alluvial deposits (Quaternary).

Ts — Tertiary sedimentary and volcanic sequence, including Butano (?) Sandstone (middle and lower Eocene), unnamed Sandstone (upper(?) and middle Miocene), Monterey Shale (middle Miocene) and Page Mill Basalt (middle Miocene).

KJf — Franciscan Assemblage (Jurassic and Cretaceous).

INTRODUCTION

A geophysical study was performed on Menlo Park Municipal Water District land and in the cities of Menlo Park and Atherton and adjoining areas. The purpose of the study was to determine the elevation of the bedrock surface beneath the flatland areas and the Stanford Linear Accelerator Center and to detect concealed faults, contacts or any other geologic structures that may affect the availability and movement of ground water. Bedrock is defined in this study to be rocks older than the Santa Clara Formation (late Pliocene and early Pleistocene). All the unconsolidated to weakly consolidated sedimentary rocks younger than and including the Santa Clara Formation are collectively refered to as "alluvial deposits" as on Sheet 2. The first part of the geophysical study involved compiling existing data, which included seismic refraction (Hazlewood, 1976), gravity (Chapman and Bishop, 1968; Fleck, 1967; Greve, 1962, Taylor, 1956), well lithologies (see Sheet 1), geologic mapping (Pampeyan, 1970), borehole gravity (Beyer, 1980), and aeromagnetic data (U.S. Geological Survey, 1971; Brabb and Hanna, 1981). The next part involved collecting and reducing additional gravity data (see Sheet 2). The third part involved measuring the density (see Sheet 2) and magnetic susceptibility of surface rock samples. The fourth and final part is described in the following text and involved synthesizing all of the pertinent data into a model of the concealed bedrock surface. This was accomplished by three-dimensional gravity modeling constrained by well, seismic, and geologic data.

GEOPHYSICAL DATA

Wells that extend to bedrock are the most direct information for determining the elevation of the bedrock surface (Sheet 1, Table 1). Wells that do not extend to bedrock provide an upper limit on the elevation of the bedrock surface. Seismic refraction interpretations by Hazlewood (1976) along profiles taken on the levees in the salt evaporator ponds north of Bayshore Freeway provide additional information with an uncertainty of about 50 feet. On Sheet 1 only the well and seismic data, in addition to geologic mapping, were used to determine the elevation of the bedrock surface at discrete locations. Then a surface of minimum curvature was used to interpolate the surface to the remainder of the study area. Sheet 3 incorporates gravity and magnetic data in the determination of the bedrock surface. Gravity and magnetic data have more continuous coverage than the well and seismic data, but a less direct relationship to the bedrock surface.

Available aeromagnetic surveys (U.S. Geological Survey, 1971; Brabb and Hanna, 1981) yield no specific information on the elevation of the bedrock surface because they were flown too high above ground (both at 3000 feet elevation). Only one magnetic anomaly, called the Redwood City anomaly by Brabb and Hanna (1981), exists in the flatland areas. Magnetic susceptibilities of various lithologies were measured in order to determine possible sources for this anomaly. The sedimentary rocks from both the Tertiary (pre-late Pliocene) units and the Franciscan assemblage are essentially non-magnetic, with susceptibilities of less than 0.1×10^{-3} cgs units. Greenstones of the Franciscan assemblage and the middle Miocene Page Mill Basalt are slightly more magnetic, with an average susceptibility of 0.1×10^{-3} cgs units. Serpentinites of the Franciscan assemblage are the most magnetic rocks exposed in the area, with an average susceptibility of 0.8×10^{-3} cgs units, ranging from 0.1 to 2.9×10^{-3} cgs units. Thus, the most likely source for the Redwood City anomaly is serpentinite. Due to its narrow, elongate shape, this anomaly could be interpreted as a faulted and/or folded serpentinite sheet (Brabb and Hanna, 1981).

There is no direct evidence that this serpentinite sheet forms part of the bedrock surface because no wells in the area of the Redwood City anomaly penetrate serpentinite. Two-dimensional (2-D) magnetic modeling of the Redwood City anomaly indicates that its source is a large serpentinite body between -1600 and -9000 feet elevation, which is below the bedrock surface elevations of -400 to -1200 feet indicated on Sheets 1 and 3. However, any short-wavelength magnetic anomalies that might be associated with serpentinite on the bedrock surface would be strongly attenuated at the 3000 foot flightline elevation; the elevation of magnetic source rocks remains uncertain. Moreover, the bedrock surface is primarily formed by non-magnetic rocks.

Bedrock surface affects the isostatic residual gravity anomaly map (Sheet 2) more than it affects the aeromagnetic data. A large density contrast exists between alluvial deposits and bedrock and variations in thickness of the alluvial deposits will cause variations in isostatic residual gravity anomalies. Gravity data provide a fairly continuous, tightly spaced ($\frac{1}{4}$-mile), areal coverage over the study area and, unlike other geophysical methods, is virtually unaffected by cultural noise problems such as electrical transmission lines, metal pipes, roads, and buildings. The main difficulty in interpreting the gravity data is separating it into its two components: the gravity related to the elevation of the bedrock surface (called the residual) and the gravity related to other geologic features (the regional). A computer modeling procedure was developed that simultaneously considers the well and seismic data and the regional/residual gravity separation problem.

RELATION OF GRAVITY TO THICKNESS OF ALLUVIAL DEPOSITS

A large amount of well and seismic data exist in the study and adjoining areas: eight $\frac{1}{2}$-mile-long seismic refraction profiles, 36 wells that penetrate bedrock, plus numerous deep wells that bottom in alluvial deposits. This control facilitates separation of the residual and regional gravity fields. Our basic premise assumes that gravity variations over alluvial deposits between well, seismic, and geologic control points are attributable to variations in the thickness of alluvial deposits. This is consistent with the assumption that short wavelengths are related to variations in thickness of alluvial deposits and that long wavelengths are related to lateral density variations in the bedrock. Then, the thickness of alluvial deposits can be modeled using the short-wavelength gravity anomalies and the elevation of the bedrock surface can be determined by subtracting the thickness of the alluvial deposits from the surface elevation.

In spite of the closely spaced well and seismic control, these assumptions are only approximations. Although the density of alluvial deposits may vary laterally, variations in thickness of alluvial deposits will be the largest contributor to shorter wavelength gravity variations. Both the shallow depth of bedrock and the large density contrast (0.2 to 0.7 g/cm^3) of alluvial deposits relative to bedrock accentuate the relationship between short-wavelength gravity variations and thickness variations. Topographic relief of the bedrock surface is nearer to the surface and, therefore, produces shorter wavelength anomalies than lateral density variations within the bedrock.

Some short-wavelength gravity variations could be expected from density variations within the alluvial deposits. For example, a local gravity low occurs over the dump site at the north end of Marsh Road. Presumably the landfill is of lower density than the surrounding alluvial deposits. However, most naturally occuring lateral density variations in the alluvial deposits probably have small density contrasts and are more localized than the dump site. Some of the very small contour wiggles or closures (one-station anomalies) in the gravity map on Sheet 2 may be attributed to local density variations in the alluvial deposits or errors in our data processing (up to 0.13 mGal rms error in the flatland areas).

COMPUTER MODELING

The purpose of the computer modeling was to determine topographic features in the bedrock surface. Errors in the model result from invalid measurements, limitations in resolution, simplifying assumptions, and uncertainties in lithological descriptions by drillers and the seismic interpretations. Nonetheless, we suggest that the general shapes of the relative lows and highs of the concealed bedrock surface are better described by the gravity modeling than by the minimum curvature method (Sheet 1). Sheet 3 shows our best estimate of the configuration of the bedrock surface given all the available data.

The computer model consists of a rectangular array of square vertical prisms. Each prism corresponds to a 512 by 512 ft (156 by 156 m) square area of the alluvial deposits. Therefore, the horizontal resolution of the model is limited to 512 ft. As a result, a few of the well and seismic data do not precisely fit the contour lines. Each prism has an assigned thickness and density contrast. The density contrast was -0.55 g/cm^3 where bedrock was assumed to be the Franciscan assemblage (based on interpretation of well lithology logs on Sheet 1) and -0.24 g/cm^3 where bedrock was assumed to be the Tertiary (pre-late Pliocene) sedimentary sequence. These contrasts were based on average density values (Table 4, Sheet 2) of 2.67 g/cm^3 for the Franciscan assemblage, of 2.36 g/cm^3 for the Tertiary sedimentary sequence, and of 2.12 g/cm^3 for the alluvial deposits. The thicknesses of the prisms are determined by the computer modeling.

The well and seismic data constrain the thicknesses of alluvial deposits at discrete points. Analogously, all bedrock outcrops were treated as alluvial deposits with zero thickness. The combination of the well, seismic, and bedrock outcrops provide control on thickness of the alluvial deposits throughout the modeling. The regional gravity, g_b, is equivalent to the gravity anomaly caused by bedrock and deeper sources. The residual gravity, g_a, is caused by the alluvial deposits. Therefore, the observed gravity anomaly, g_o is:

$$g_o = g_a + g_b. \tag{1}$$

In the computer procedure, an initial model of the alluvial deposits based on the well, seismic, and contact data was determined by fitting a surface of minimum curvature between the control points, much like in Sheet 1. The gravitational effect of this model, g'_a, was calculated as an initial estimate of g_a. Then, by equation (1), an estimate of the gravitational effect of the bedrock, g'_b, would be:

$$g'_b = g_o - g'_a. \tag{2}$$

We note that g'_a is not a very good estimate of g_a between the control points because g'_a was calculated from the smooth, initial thickness model of the alluvial deposits, and is, therefore, also smooth. In fact, from equation (2) the shorter wavelength portion of g_o remains in g'_b, and g'_b is a poor estimate of g_b between the control points. However, g'_b is a good estimate of g_b at the control points. We expect g_b to vary smoothly because of its deeper density sources. We then fit a surface of minimum curvature through g'_b at these locations, obtaining g''_b. A new estimate of g_a, g''_a, which contains the shorter wavelength gravity variations, is given by

$$g''_a = g_o - g''_b. \tag{3}$$

Next, the thickness of a prism, t, is adjusted to a new thickness, t', by the iterative procedure of Cordell and Henderson (1968):

$$t' = t\,\frac{g''_a}{g_a}. \tag{5}$$

After this adjustment, the gravitational effect of the new alluvial model is calculated, the new model is treated as an initial model, and the above process is repeated. Convergence of the observed and calculated gravity was achieved after six iterations.

RESULTS

The primary differences between the contours in Sheet 1 and Sheet 3 are found between the well, seismic, and geologic control points because Sheet 3 is based on the assumption that gravity variations between well control points are attributable to variations in thickness of alluvial deposits. None of the faults on Sheet 3 are known to be associated with seismic or aseismic hazards.

Both Sheet 1 and Sheet 3 show bedrock surface to be deepest on the eastern edge of the quadrangle, which corresponds to the northwestern edge of the Santa Clara Valley ground water basin (Department of Water Resources, 1975). Wells penetrating bedrock at -880, -875, -940, and -1024 feet elevation, in addition to a well that does not penetrate bedrock at -1058 ft elevation define this low. This feature differs on Sheet 3 from that on Sheet 1 because the bedrock surface on Sheet 3 follows a clearly defined gravity low toward East Palo Alto. The gravity low extends southeast to the -1058 ft elevation well, but is centered in East Palo Alto where there is no deep well control.

To the northwest, this gravity low connects with a northwest striking gravity trough. The southwest boundary of this gravity trough is defined by a very linear gravity gradient, indicating a planar contact, such as a fault. We have inferred the Palo Alto fault on maximum values of the horizontal gravity gradient (Blakely and Simpson, 1986). Taylor (1956) previously inferred the presence of the Palo Alto fault from this gravity feature, defined at that time by far fewer gravity stations, located less than 500 feet away from our location. The gravity trough is also apparent as a bedrock gravity low, indicating that it cannot be entirely explained by alluvial deposits, and that a relatively low-density lithology occurs in the bedrock (Franciscan assemblage) at this location. The southwestern contact occurs in virtually the same position on both the observed and bedrock maps which indicates that this fault is related to a contact between two lithologies within the bedrock. The northeast side of the trough, controlled by a profile of gravity stations along the Dumbarton Bridge approach, may define another fault. The Redwood City magnetic anomaly (Brabb and Hanna, 1981) coincides with this gravity low. Given the tendency of serpentinite to occur along zones of weakness, Brabb and Hanna (1981) inferred the Redwood City fault along the center of this magnetic anomaly, roughly half-way between and parallel to the two gravity-inferred faults. Our gravity and magnetic modeling indicates that a large serpentinite body lies continuously between these two faults and is overlain by graywacke and shale of the Franciscan assemblage. We here define the Redwood City fault zone, which includes the inferred serpentinite body, the Redwood City fault inferred by Brabb and Hanna (1981), the Palo Alto fault originally inferred by Taylor (1956), and our gravity-inferred fault near the Dumbarton Bridge approach.

A distinct, northwest-southeast depression in the bedrock surface occurs in south-central Atherton. This feature does not appear on Sheet 1. The low is related to a gravity trough bounded to the northeast by a sharp gravity gradient that extends from near Selby Lane School in Redwood City to the Academy of the Sacred Heart in Atherton (Sheet 2). The bedrock surface depression is elongated parallel to fold axes in Eocene rocks mapped by Pampeyan (1970) about 1.5 miles to the southeast. The Santa Clara Formation (included herein within the alluvial deposits) is also folded parallel to the Eocene rocks. Therefore, the depression may be a buried syncline composed of the Santa Clara Formation. A possible valley on the bedrock surface located just north of Las Lomitas School in southern Atherton described on Sheet 1 appears to be less extensive on Sheet 3, where it is overwhelmed by the buried syncline. Perhaps this "valley" is a former ravine along the former, now buried, escarpment of the hills above Menlo Park and Atherton. A creek following this ravine may have drained into a valley along the buried syncline.

The gradient northeast of the possible buried syncline was previously interpreted as a fault by Taylor (1956) on the basis of gravity data available at that time. On the basis of our more detailed gravity coverage, we have relocated this inferred fault, which we call the Atherton fault on Sheet 3. Our location was inferred from the horizontal gradient of gravity anomalies. Large maximum horizontal gravity gradient values occurred in virtually the same position on the "bedrock" gravity map, indicating that the Atherton fault corresponds to a significant density contrast within the bedrock, such as the -0.31 g/cm^3 contrast between the Tertiary (pre-late Pliocene) sequence and the Franciscan assemblage. Therefore, the Atherton fault probably defines a steep contact between the Tertiary sequence to the southwest and the Franciscan assemblage to the northeast (see profiles AA' and BB'). A contact between these geologic units in this vicinity is supported by the well information on Table 1, Sheet 1. The Atherton fault may join a steeply dipping fault dividing serpentinite to the north and Eocene rocks to the south in the area near Arroyo Ojo de Agua (Pampeyan, 1970), or it may join an exposed shear zone to the northwest (Brabb and Pampeyan, 1983) that divides the Tertiary sequence and the Franciscan assemblage. The fact that a shear zone divides the nearest exposures of the contact between the Tertiary sequence and the Franciscan assemblage supports the idea that a fault (or shear zone) forms the extension of this contact beneath Atherton and Menlo Park.

The gravity gradient that defines the Atherton fault is progressively weaker as it approaches San Francisquito Creek in a southeasterly direction, indicating that the fault is splayed, splintered, or offset. Our projected trace of the Atherton fault terminates at an interpreted left-lateral "tear" fault, which we here call the San Francisquito fault. This inferred fault trends southwest-northeast and may have about 1 mile of left-lateral offset. Its location is also based on maximum values of the horizontal gravity gradient. The location and left-lateral displacement of the San Francisquito fault are supported by two geologic features: (1) other left-lateral faults that displace the contacts between Eocene and Miocene sedimentary rocks (Pampeyan, 1970) exposed near Sand Hill Road are colinear with the San Francisquito fault, and (2) between these left-lateral faults and the San Francisquito fault, the Pulgas fault becomes a shear zone and is bent in a left-lateral sense. If the Atherton fault extends to the southeast beyond the San Francisquito fault, its location is uncertain due to lack of gravity and well data in the Palo Alto area. The San Francisquito fault is aligned along the northern edge of a northeast trending depression in the bedrock surface located slightly southeast of the present drainage of San Francisquito Creek. Several wells below -500 feet elevation control the bedrock surface along the depression. The gravity modeling indicates that the depression trends about N 45° E from the well that penetrates bedrock at -537 ft elevation, compared to a trend of about N 30° E on Sheet 1.

Other notable features revealed by the gravity modeling are two northwest-southeast trending ridges located near the center of the study area: one about 1 mile south of the Bayshore Freeway in Atherton, and one just north of the Atherton fault. The possible buried ridges are parallel to the pervasive, roughly N 40-60° W trends of other exposed ridges, faults, and fold axes in the area. A depression situated between these two ridges appears to slope northwest toward Garfield School in Redwood City, then turns northward to Fair Oaks School. A depression centered between Encinal School, Nativity School, and Menlo School and College in west Menlo Park is part of a buried basin with an area of about 1 mi^2. Streams from a ravine near Las Lomitas School and the buried syncline may have drained into this basin, then east toward the depression southeast of the San Francisquito fault or, perhaps, the depression by Garfield School in Redwood City. North of the Bayshore Freeway, where the model is largely controlled by the seismic refraction lines, local bedrock highs and lows are defined, but no drainages are recognized.

The Pulgas fault, the Belmont Hills fault, and the fault located near Hanover Street were located or inferred from geologic mapping. No continuous linear gravity gradients were found in association with these faults. This implies that either (1) not enough gravity data were collected to define the gravity gradients associated with these faults or (2) a significant density contrast does not exist in the bedrock across the fault contact. Reason (2) applies to the Pulgas fault in Menlo Park and Atherton, where the Tertiary (pre-late Pliocene) sequence forms the bedrock on both sides of this fault. Reasons (1) or (2) could apply to the remaining part of the Pulgas fault, the Belmont Hills fault, and the fault located near Hanover Street in Palo Alto, which are all outside of the study area.

Profiles AA' and BB' were constructed based on the information shown on Sheet 3 and Table 1, Sheet 1. They are located along the same lines as the profiles constructed by the Barrett Consulting Group (1989). The dips of the inferred faults are not known, but the two sets of blocks marking the Pulgas and Atherton faults denote the limits of uncertainty of 90° ±45° in the angle of the fault dip based on gravity modeling. Wells near each profile were projected on to the profile to emphasize their control on the bedrock surface.

CONCLUSION

The assumptions used to contour Sheet 1 and Sheet 3 between well control points yielded different results. The mathematical assumption of minimum curvature was made to construct Sheet 1; Sheet 3 was constructed by assuming that shorter wavelength gravity anomalies are related to variations in thickness of alluvial deposits. Some of the short wavelength gravity anomalies alternatively could be explained by lateral density variations in the alluvial deposits or the bedrock. The resulting map of the configuration of the bedrock surface shown on Sheet 3 has revealed some interesting features, such as faults, buried valleys, a synclinal feature, ridges, and depressions. All of these features are supported by either well information, exposed geology, or the general tectonic setting of the area. Therefore, Sheet 3 may provide valuable information for siting wells and for studying and obtaining ground water.

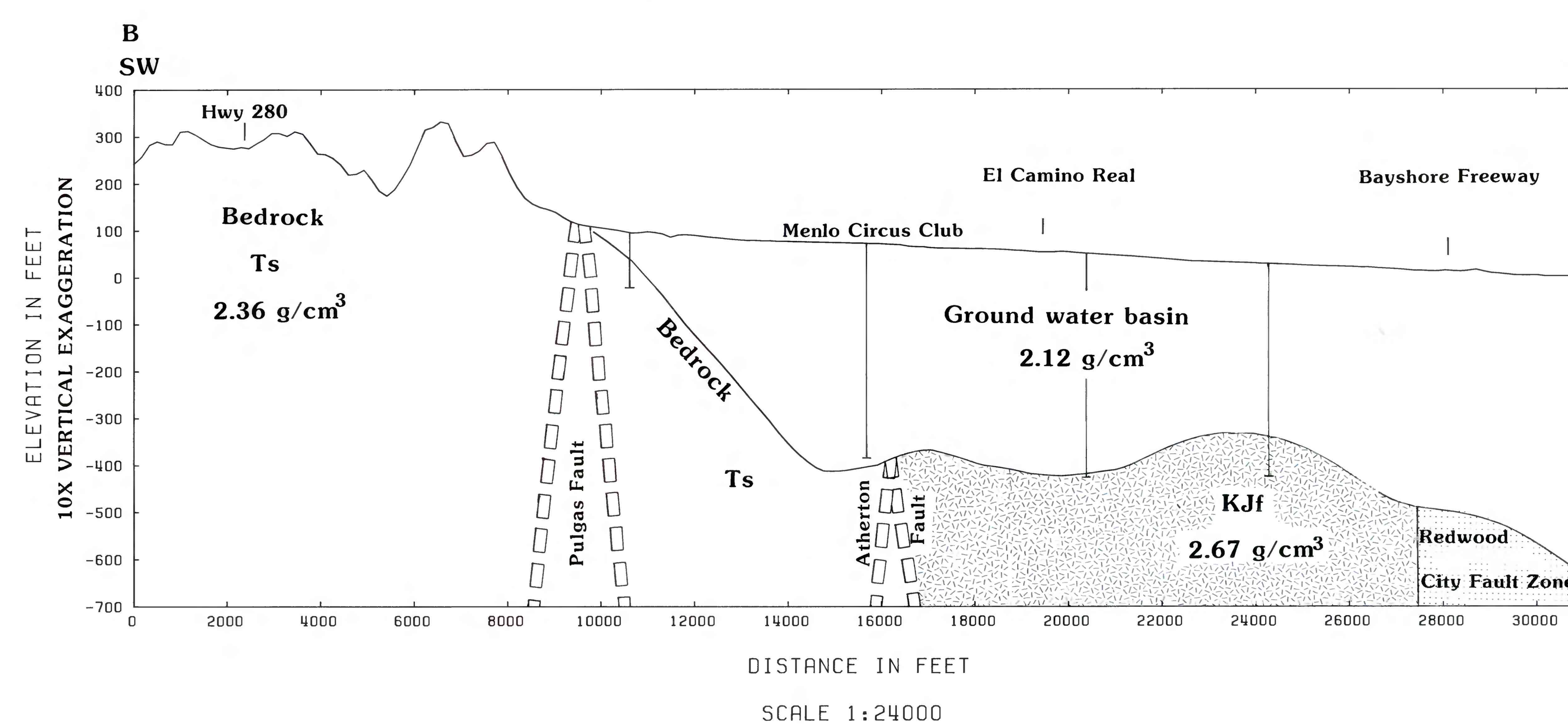

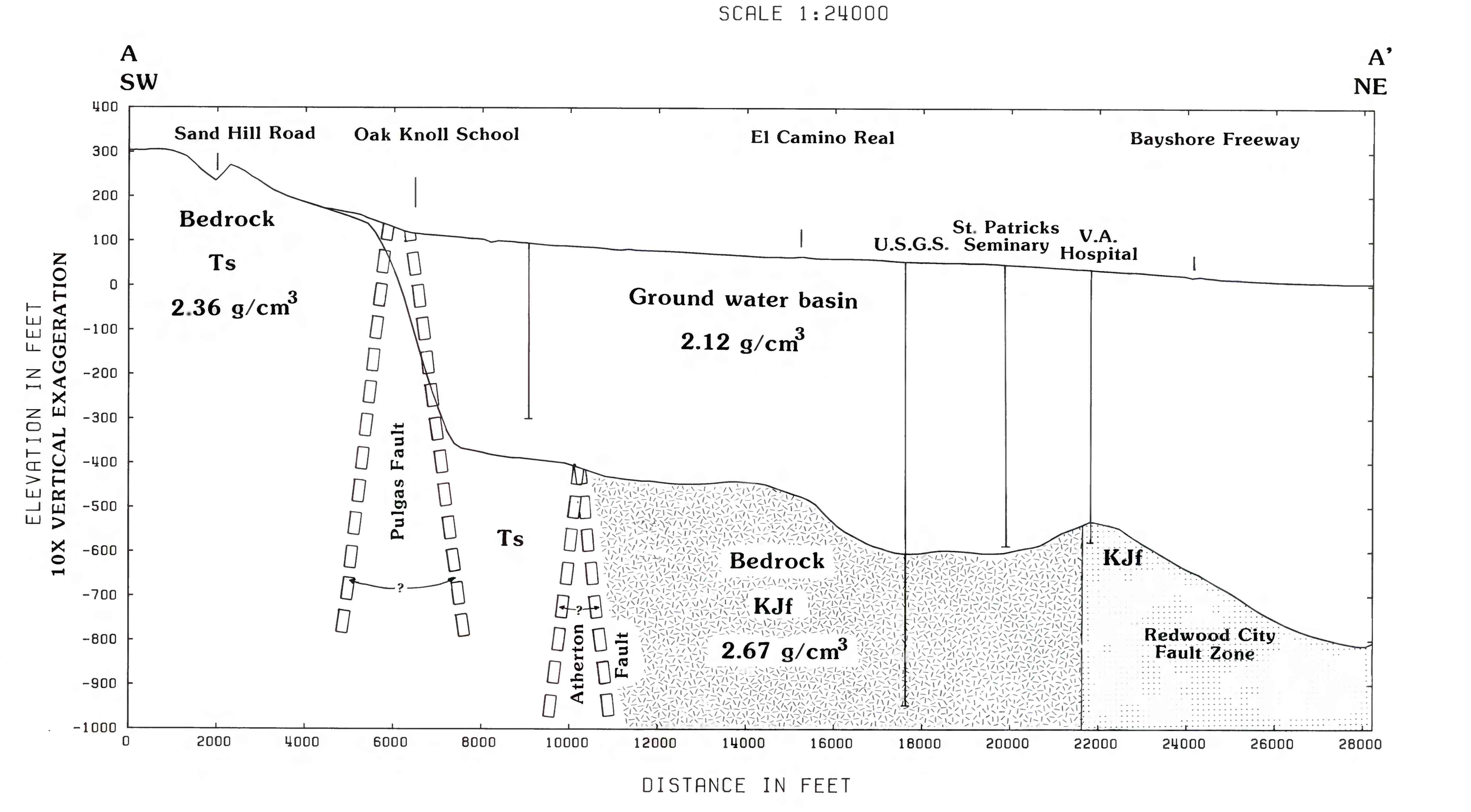

REFERENCES (SHEET 3)

Barrett Consulting Group Inc., 1989, Groundwater supply and system storage investigation for the City of Menlo Park: Barret Consulting Group Inc., Menlo Park, CA, unpub. report.

Beyer, L.A., 1980, Borehole gravity program of the U.S. Geological Survey (1963-1975)–brief history and basic data: U.S. Geological Survey Open-File Report 80-903.

Blakely, R. J., and Simpson, R. W., 1986, Approximating edges of source bodies from magnetic or gravity anomalies: Geophysics, v. 51, p. 1494-1498.

Brabb, E. E., and Hanna, W.F., 1981, Maps showing the aeromagnetic anomalies, faults, earthquake epicenters, and igneous rocks in the southern San Francisco Bay region, California: U.S. Geological Survey Geophysical Investigations Map GP-932, scale 1:62,500.

Brabb, E. E., and Pampeyan, E. H., 1983, Geologic map of San Mateo County, California: U.S. Geological Survey Miscellaneous Investigations Map I-1257-A, scale 1:62,500.

Chapman, R. H., and Bishop, C. C., 1968, Bouguer gravity map of California -San Francisco sheet: California Div. Mines and Geology, 3 p., 1 map, scale 1:250,000.

Cordell, L., and Henderson, R. G, 1968, Iterative three-dimensional solution of gravity anomaly data using a digital computer: Geophysics, v. 33 p. 596-601.

Department of Water Resources, 1975, Evaluation of ground water resources: South San Francisco Bay: Bull. 118-1, v. 3, Northern Santa Clara County area, 133 p.

Fleck, R. J., 1967, Structural significance of the contact between Franciscan and Cenozoic rocks, southern San Francisco Peninsula, California: Stanford Univ., Unpub. Student Research Project, 6 p.

Greve, G. M., 1962, An investigation of the earth's gravitational and magnetic fields on the San Francisco Peninsula, California: Stanford Univ., [Unpub.] Ph.D. thesis, Stanford, California, 209 p.

Hazlewood, R. M., 1976, Contour map and interpretive cross sections showing depth and configuration of bedrock surface, south San Francisco Bay region, California: U.S. Geological Survey Miscellaneous Field Studies Map MF-796, 2 sheets, map scale 1:62,500.

Pampeyan, E.H., 1970, Geologic map of the Palo Alto 7-1/2-minute quadrangle, San Mateo and Santa Clara Counties, California: U.S. Geological Survey Open-File Map 70-254, scale 1:12,000.

Taylor, S. G., Jr., 1956, Gravity investigation of the southern San Francisco Bay area, California: Stanford Univ., Ph.D. thesis, 105 p.

U.S. Geological Survey, 1971, Aeromagnetic map of the southern part of the San Francisco Bay region, California: U.S. Geological Survey Open-File Report 71-294, scale 1:125,000.